XXXVI Ibero-Latin American
Congress on Computational
Methods in Engineering
CILAMCE
Rio de Janeiro, 22-25 Nov 2015

NUMERICAL MODELLING OF FOUR-POINT BENDING TEST USING COHESIVE FRACTURE MODELS

Machado, William G.

Mejia Sanchez, E. C.

Roehl, Deane

williamgmachado@gmail.com

crisms@tecgraf.puc-rio.br

droehl@puc-rio.br

Instituto Tecgraf e Departamento Engenharia Civil PUC-Rio

Rua Marques de São Vicente, 225, Gávea, 22453900, Rio de Janeiro, RJ, Brasil.

Abstract. *The bending test has become an important test method for concrete to determine the material properties and tensile strength, as well as to predict the mixed-mode crack path. In this work, cohesive models are used to simulate fracture in a four-point bending test. Two cohesive models are compared: a potential-based cohesive zone model proposed by Paulino et al. and a linear model proposed by Camanho, et al. Experimental results obtained by Galvez for a concrete beam, using a novel bending test procedure, are regarded as reference results. This procedure allows submitting the test specimen to non-proportional loading, generating different crack paths by changing the action of an actuator. The tests were performed for two specimen sizes and two mixed-mode loading conditions. The numerical results such as curves of load-CMOD and load-transversal displacement were compared with the experimental results. The evaluation of the performance of these cohesive models is very important aiming at the study of complex problems in order to predict critical loads, stress/strain behavior in post-critical regime and crack paths under mixed-mode conditions. The numerical results show that cohesive elements can be used as an attractive alternative to model mixed-mode fracture.*

Keywords: *Cohesive fracture, four-point bending, mixed-mode fracture, finite element method*

1 INTRODUCTION

The numerical modelling of fracture process in materials with softening behavior is a complex problem. In the last two decades, a lot of work has been carried out in order to develop analytical and numerical models to describe the initiation and propagation of the cracks. The numerical methods based on the finite element to simulate fracture process can be classified in two groups: the smeared and the discrete crack models. The main idea of the smeared crack model is to spread the energy release along the width of the localization band within a single element. Theoretically, an infinite number of parallel microcracks are distributed over the finite element. However, this model presents some difficulties such as mesh alignment sensitivity, localization instabilities and a possible ill-posed equation system (Rabczuk, 2013). In order to overcome these problems, other strategies were developed, such as the non-local continuum model and the crack band model proposed by Bazant (Bazant & Oh, 1983; Bazant & Pijaudier-Cabot, 1988).

The discrete crack model is recommended when there is either a distinct crack or a finite number of cracks. In this model, the crack is introduced as a geometric entity. Among the possibilities to include discrete cracks in the numerical simulations are the cohesive elements, introduced geometrically along the predefined crack path at the beginning of the simulation. Alternatively, cracks can be introduced by adding degrees of freedom with a jump function to the finite element displacement field. The Extended Finite Element Method (XFEM) follows this type of formulation.

The cohesive crack model introduced by (Barenblatt, 1962 and Dugdale, 1960) relates the traction across the crack surfaces to the displacement jump around the crack head. Damage initiation is related to the maximum strength or separation. The area under this curve represents the fracture energy and the crack is formed when the traction is reduced to zero (Gonzalvez et al. 2009). An important aspect in the cohesive zone model is the choice of traction-separation law because some relations show limitations, especially under mixed mode conditions. For example, the potential-based cohesive model “PPR” proposed by (Park, et al. 2008) defines the traction-separation law from a potential function. This model was successful by the simulation of problems under mixed-mode conditions. An alternative traction-separation law is given by the linear cohesive model proposed by (Turon and Camanho, 2006).

The combination of a tensile/shear failure (mode I and II) is known as mixed-mode fracture (Reyes et al. 2008). The simulation of a mixed-mode fracture found several difficulties to be modelled because it requires an input of material properties which are difficult to evaluate, such as softening function and fracture energy in mode II (Cedon, et al. 2000). The following studies developed by (Galvez, et al 1996, Galvez, et al 1998; and Galvez, et al 2002) show the experimental results of a four-point bending test. This testing procedure was successfully used for a mixed mode fracture of concrete. The experimental result records the load-displacement of several control points for three sizes of the specimen test.

In this work, both the PPR cohesive model and the bi-linear cohesive model are used to simulate fracture in a four-point bending test. To allow for an arbitrary direction of crack propagation, the cohesive elements are introduced between the continuum elements in the zone of interest. The numerical results such as load-CMOD and load-transversal displacement curves were compared with the experimental results obtained by Galvez. In the following section, the linear damage constitutive model and the potential-based cohesive zone model (PPR) will be explained.

2 COHESIVE CRACK MODEL

In the zone of fracture process, the cohesive tractions are related to their separation jump through a specific relationship. This relationship is given by the following expression (Potts and Zdravkovic, 1999).

$$\sigma_i = D_{ij}.\Delta\delta_j \tag{1}$$

where D_{ij} is the tangential constitutive matrix that depends on the traction-separation relationship such as the potential function and the linear softening model.

2.1 Linear cohesive model

This cohesive model is represented by a bilinear relationship. This relationship assumes a linear elastic behavior until the critical point of damage initiation, where the traction reaches the maximum cohesive stress $T_{\max}$ and the separation reaches the value of δ_o, followed by the linear softening behavior characterized by progressive degradation of the material stiffness. The new crack is created when the separation reaches the critical value of δ_f and the cohesive traction becomes zero. The area under the traction-separation curve is equal to the fracture energy Gc, as shown in Fig. 1 (Gonzalez et al. 2009, Bendezu et al., 2013 and Mejia et al. 2015)

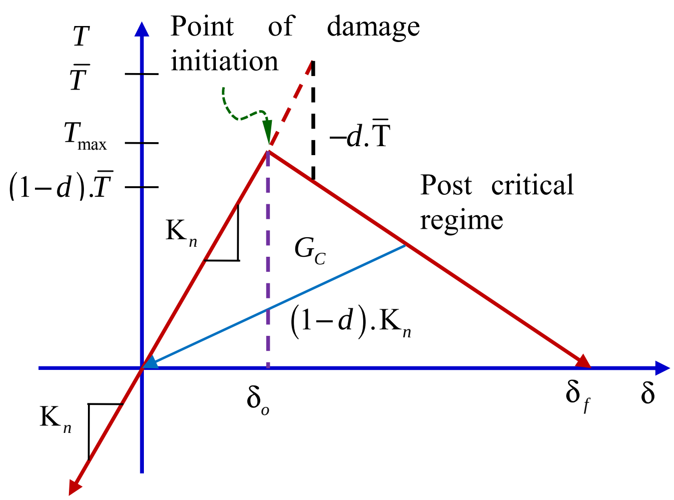

Figure 1. Typical response of cohesive element with linear softening (Mejia et al, 2015)

The cohesive traction T_i shown in Fig. 1 can be defined as,

$$T_i = \begin{cases} K_n.\delta & \Leftarrow \quad \delta \le \delta_o \\ (1-d).K_n.\delta & \Leftarrow \quad \delta_o < \delta < \delta_f \\ 0 & \Leftarrow \quad \delta \ge \delta_f \end{cases} \tag{2}$$

where K_n is the normal elastic stiffness and d the damage variable. In post-critical regime for linear softening, the damage variable is defined as (Davila, et al. 2007, Turon et al. 2006),

$$d = \frac{\delta_f.(\delta_m - \delta_o)}{\delta_m.(\delta_f - \delta_o)} \tag{3}$$

where $\delta_m = \sqrt{\langle \delta_n \rangle^2 + \delta_s^2}$ is the maximum value of effective displacement.

2.2 Potential-based cohesive zone model

The PPR cohesive model proposed by (Park et al, 2008) uses a potential function as the relationship between cohesive traction and relative displacement. The PPR potential function of cohesive fracture is given by,

$$\psi(\Delta_n, \Delta_t) = \begin{cases} \min(\phi_n, \phi_t) + \left[\Gamma_n.\left(1 - \frac{\Delta_n}{\delta_n}\right)^{\alpha}.\left(\frac{m}{\alpha} - \frac{\Delta_n}{\delta_n}\right)^{m} + \langle \phi_n - \phi_t \rangle \right]. \\ \left[\Gamma_t.\left(1 - \frac{|\Delta_t|}{\delta_t}\right)^{\beta}.\left(\frac{n}{\beta} - |\Delta_t|.\delta_t\right)^{n} + \langle \phi_t - \phi_n \rangle \right] \end{cases} \tag{4}$$

where ϕ_n is the normal fracture energy, ϕ_t the tangential fracture energy, Δ_n the normal separation, Δ_t the tangential separation, δ_n the normal final crack opening, δ_t the tangential final crack opening, Γ_n, Γ_t the energy constants, α, β the shape parameters and m, n the exponents of the PPR model.

The normal and tangential cohesive tractions are obtained by the derivatives of the PPR potential function with respect to the normal and tangential separations.

$$\left.\begin{aligned} T_n(\Delta_n, \Delta_t) &= \partial\psi(\Delta_n, \Delta_t)/\partial\Delta_n \\ T_t(\Delta_n, \Delta_t) &= \partial\psi(\Delta_n, \Delta_t)/\partial\Delta_t \end{aligned}\right\} \tag{5}$$

The parameters α and β define the shape of cohesive traction curve and allow the representation of various material softening response curves, as shown in Fig. 2.

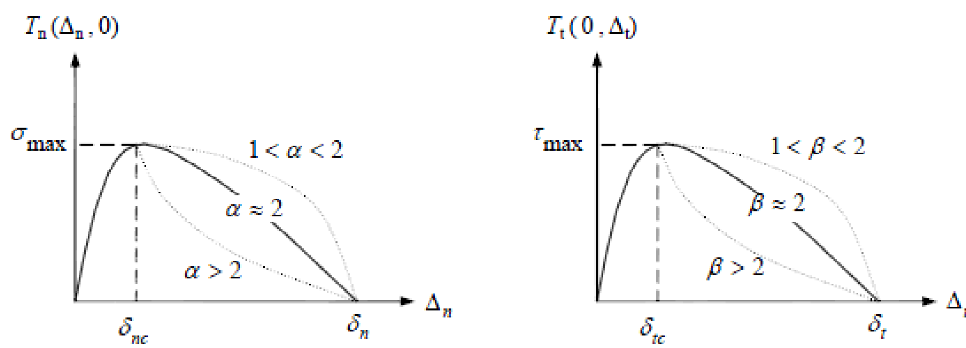

Figure 2. Influence of the shape parameters of cohesive traction responses (Park et al, 2008)

This cohesive model was implemented by (Park et al. 2012) as a UEL subroutine in Abaqus.

2.3 The Criterion of damage propagation for a mixed mode fracture

The propagation criterion for a fracture process under mixed-mode loading condition is established according to the components of the energy release rates. The criterion proposed by (Benzenggagh and Kenane, 1996) is widely used to predict crack propagation under mixed-mode loading. This criterion is expressed as,

$$G_{Ic} + \left(G_{IIc} - G_{Ic}\right).\left(\frac{G_{II}}{G_1 + G_{II}}\right)^{\eta} = G_c \tag{6}$$

Where G_c is the critical energy release rate, η is a material parameter, G_I and G_{II} are the energy release rates in mode I e II, respectively, while G_{Ic} and G_{IIc} are the fracture toughness in mode I and II, respectively. The parameter η is found by fit of experimental data of the energy toughness under different mixed-mode ratios.

In this work, the BK- criterion is used along with a linear cohesive model. On the other hand, the PPR model for mixed-mode fracture is associated to the potential function by the physical macroscopic fracture parameters (Park et al. 2008).

3 TESTING PROCEDURES AND PROPERTIES

3.1 Four-point bending test

Two models were simulated in a computer program for the mixed-mode fracture analysis, according to Galvéz (1998) experiment. Figure 3a and 3b show the geometry, the loading procedure and the boundary conditions of these models and the dimensions are detailed in Table 1. The force P was supplied by an independent actuator, which permits non proportional loading of the experiment.

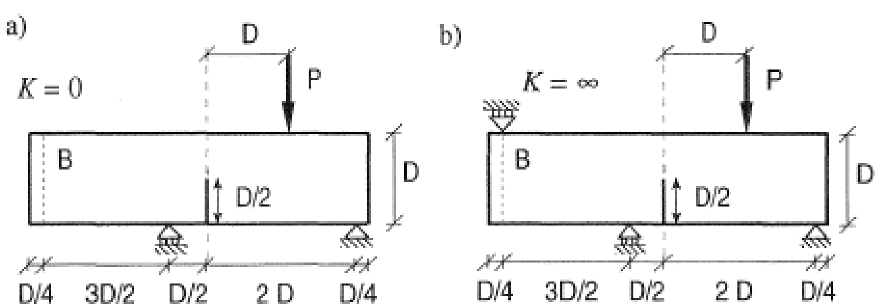

Figure 3. Geometry, boundary conditions and force diagrams under non proportional mixed mode tests. (a) Type 1 (K = 0), (b) Type 2 (K = ∞) (Galvéz et al. 1998).

Table 1. Dimensions of specimens.

	D (mm)	L (mm)	B (mm)
D1	75	340	50
D2	150	675	50

D: Depth
L: Length
B: Thickness

In addition, different values of the spring stiffness and combinations of P and distance D were adopted, in each model, to provide different trajectories of the crack. The extreme values used were K = 0 in type 1 tests Fig. 3a and in type 2 testes, K was ∞ Fig. 3b. Type 1 tests were performed without displacement control at point B. In type 2 tests, the boundary condition at point B prevents vertical displacement throughout the test.

During the tests, the following parameters were recorded: the CMOD, the load P, the load-point displacement of force P, the displacement of point B (test type 1) and the reaction force at point B (type test 2) and the results were compared with those from the experimental tests made by Galvéz (1998).

3.2 Material and specimens

In this work, the first batch of experiments carried out by Galvéz (1998) was used in order to simulate the numerical prediction of the crack path using a linear cohesive model and a PPR model. The mechanical properties of the mixture, cohesive linear parameters and PPR parameters are given in Tables 2, 3 and 4, respectively. These parameters were adjusted from the experimental properties for each cohesive model.

Table 2. Mechanical properties of the mixture (Galvez1998).

E (GPa)	ν	G_c (N/m)	fck (MPa)	fct (MPa)
38	0.2	69	54	3.0

Table 3. Linear cohesive parameters.

σ_n (MPa)	τ (MPa)	K_n (MPa)	K_t (MPa)	G_c (N/m)
3.0	3.0	$3.8 \cdot 10^4$	$1.62 \cdot 10^4$	69

Table 4. PPR parameters.

$Ø_n$ (N/m)	$Ø_t$ (N/m)	σ_{max} (MPa)	τ_{max} (MPa)	α	β	Ψ_n	Ψ_t
69	69	3.0	3.0	5.0	5.0	0.005	0.005

4 NUMERICAL MODELS AND NUMERICAL RESULTS

In this work mixed mode fracture of concrete beams is investigated through cohesive crack models. The investigation consists in predicting the crack path for the tests procedures and specimen sizes defined in Figure 3 and Table 1, respectively. Crack propagation is predicted by the maximum principal stress criterion. The numerical simulations were run using ABAQUS® software. The control of the non-linear analysis is based on the Riks method, which is widely employed in the simulation of softening materials such as concrete.

4.1 Numerical results of test Type 1

In Type 1 models, two different model sizes were simulated. The small specimen has D1 = 75mm and the medium specimen has D2 = 150 mm, see Figure 3. Figures 4 and 5 show the experimental envelopes from Galvéz (1998) and the numerical predictions calculated with ABAQUS ® for each specimen size.

Figures 4a and 5a show the records of the trajectory of the cracks; Fig. 4b and 5b show the Load P vs. CMOD; Fig. 4c and 5c show the load P vs. load-point vertical displacement and Fig 4d and 5d show the load P vs. point B vertical displacement curves.

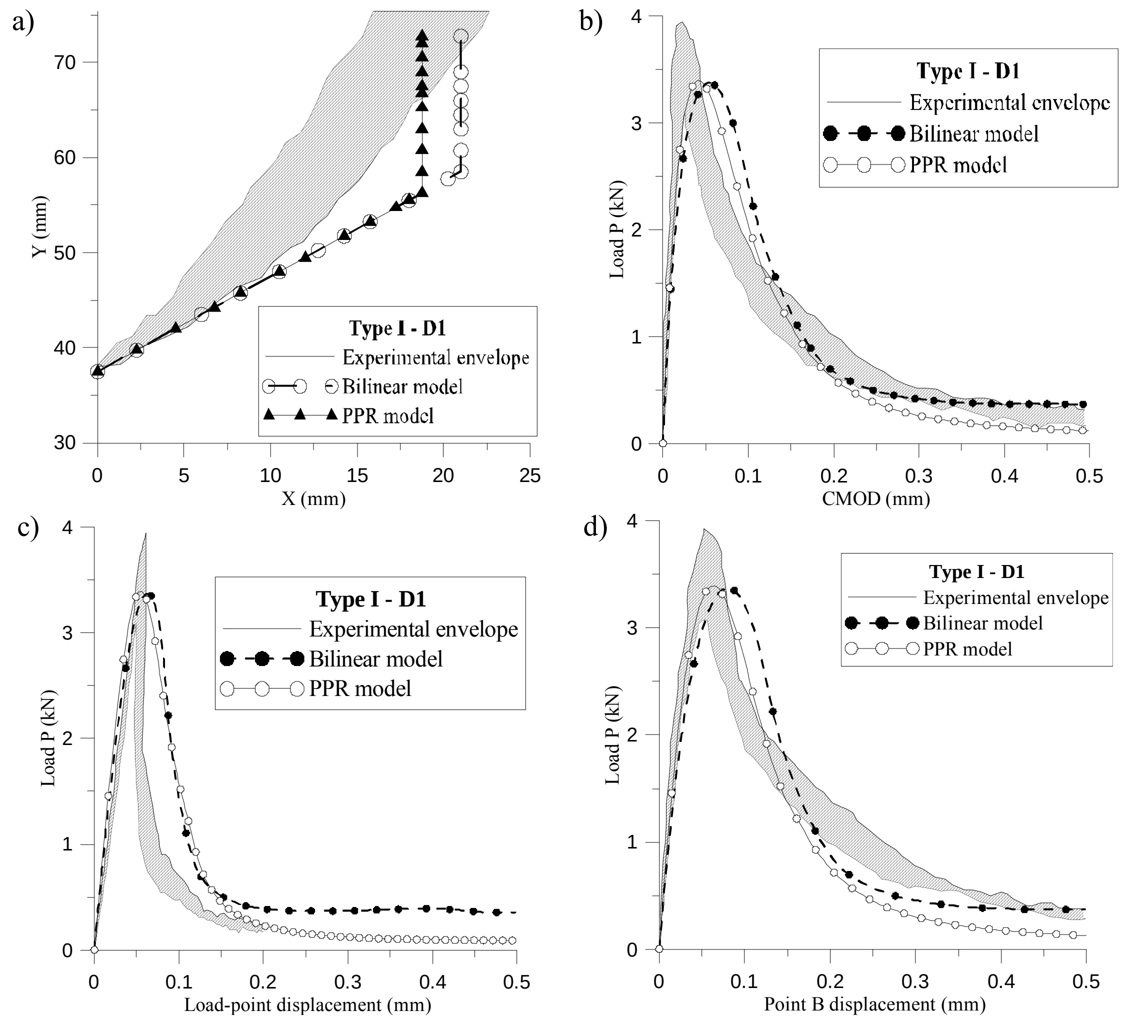

Figure 4. Numerical results for model type 1 - D1=75 mm a) crack trajectory b) Load P vs CMOD c) load P vs. load point vertical displacement and d) load P vs. vertical displacement of point B.

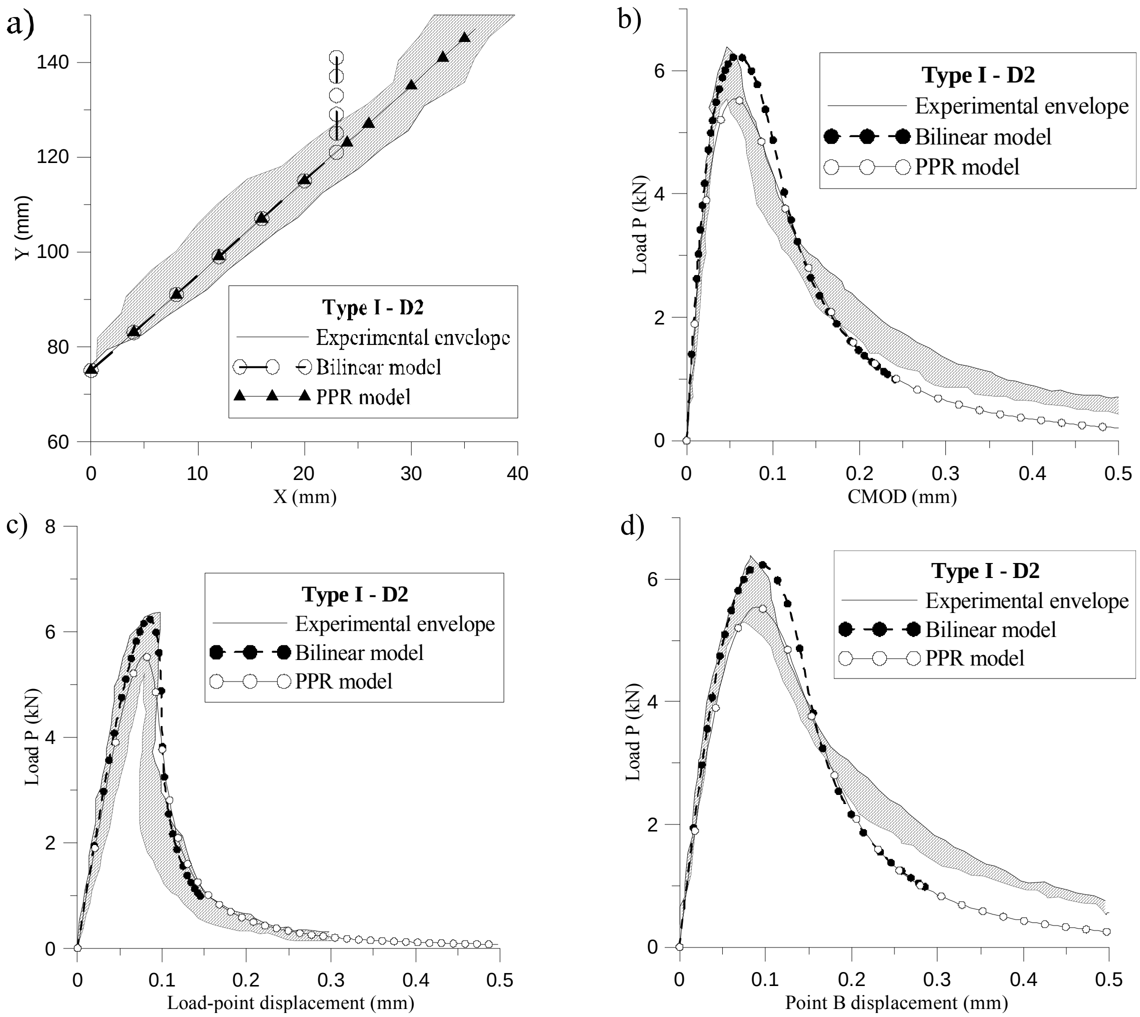

Figure 5. Numerical results for model type 1 - D2=150 mm a) crack trajectory b) Load P vs CMOD c) load P vs. load point vertical displacement and d) load P vs. vertical displacement of point B.

4.2 Numerical result of test Type 2

In Type 2 models, two different model sizes were simulated. The small specimen has D1 = 75mm and the medium specimen has D2 = 150 mm. Figures 7, 8 and 9 show the experimental envelopes from Galvéz (1998) and the numerical prediction calculated using ABAQUS ® for each size.

Figures 6a and 7a show the records of the trajectory of the cracks; Fig. 6b and 7b show the load P vs. CMOD; Fig. 6c and 8a show the load P x load-point vertical displacement and Fig. 6d and 8b show the reaction at point B x CMOD curves.

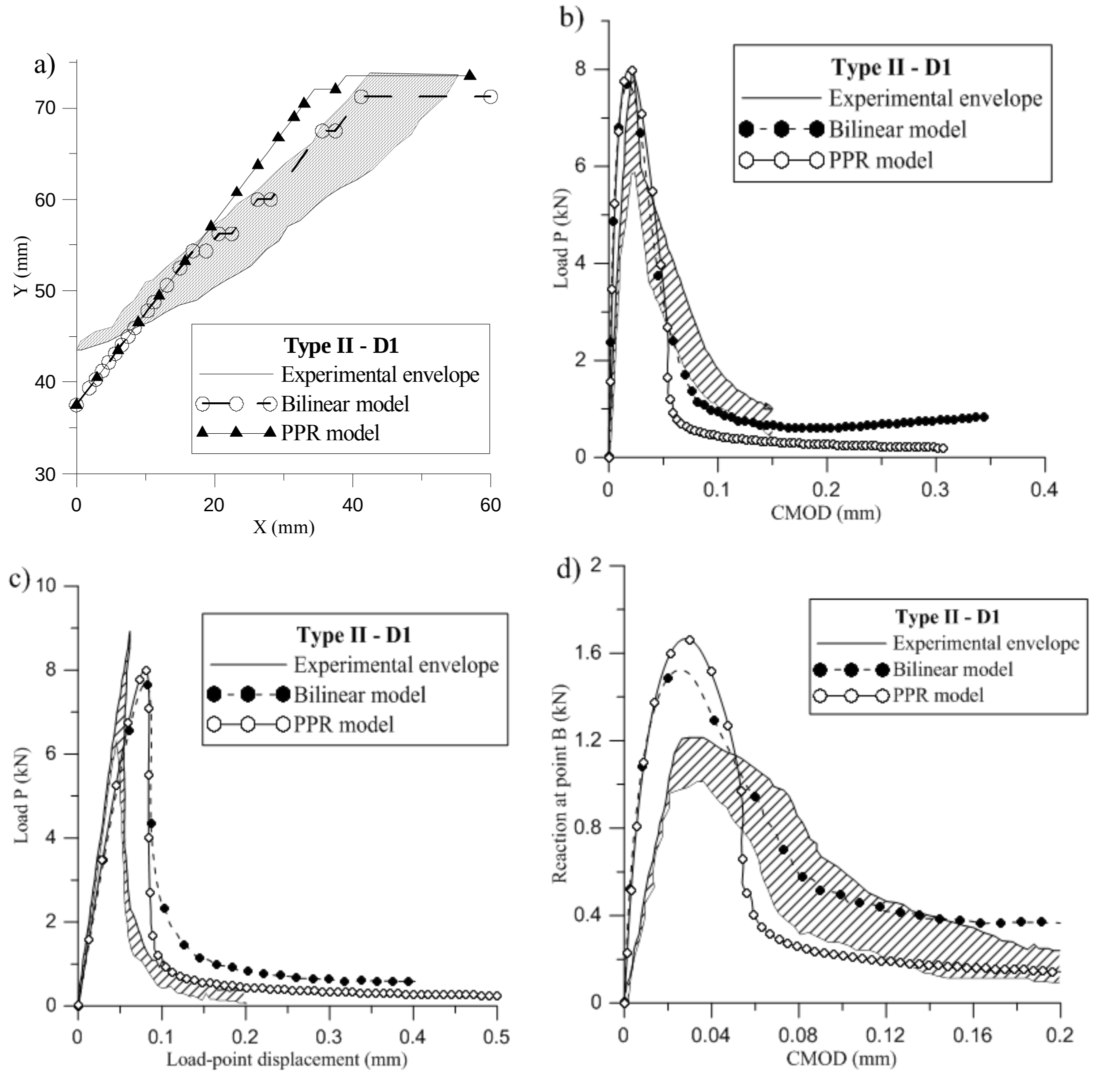

Figure 6. Numerical results for type 2 - D1=75 mm a) crack trajectory b) load P vs CMOD c) load P vs. load point vertical displacement and d) reaction at point B vs. CMOD.

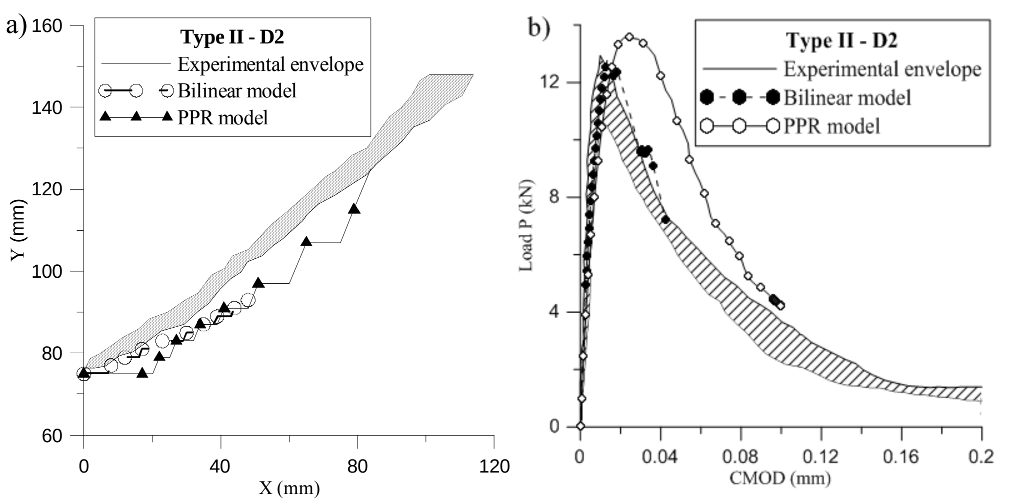

Figure 7. Numerical results for type 2 – D2=150 mm a) crack trajectory b) load P vs CMOD

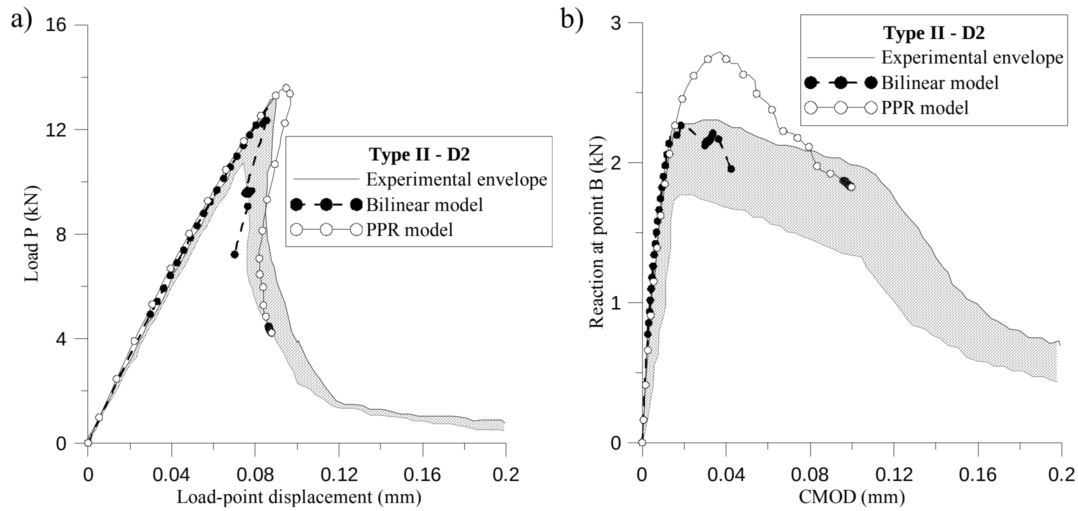

Figure 8. Numerical results for type 2 – D2=150 mm a) load P vs. load point vertical displacement and b) reaction at point B vs. CMOD.

5 CONCLUDING REMARKS

The experimental results presented in this work are used to validate the numerical result of cohesive fracture models. The numerical model predicts the crack trajectories and records the loads and displacements at several control points of the specimen test for two sizes of specimen and two mixed-mode loading conditions.

For the numerical modeling, cohesive elements are included between the continuum elements in the zone of interest. The results obtained using cohesive crack models are in good approximation with the experimental crack path for concrete structures, even though the fracture behavior is clearly nonlinear. According to the predicted crack path in Fig. 8a and 9a, the PPR model demonstrates its capacity and robustness to model mixed-mode conditions.

According to the numerical results of type 1 test, the agreement is good for both linear and PPR models, especially in the ascending branch of the curve. The peak load is well predicted in most cases and the descending branch is a good approximation, since it is close to the experimental envelope. In the type 2 test, the agreement of the ascending branch is good in most cases and the peak load is also well predicted. The descending branch of the curves is a good approximation, especially in linear models. Since the crack must follow the cohesive element path, the predicted trajectory is jagged. Mesh refinement would reduce this effect.

ACKNOWLEDGEMENTS

This research was carried out in Tecgraf Institute/PUC-Rio.

REFERENCES

Barenblatt, G. I., 1962. The mathematical theory of equilibrium crack in brittle fracture. In: *Advanced Applied Mechanics*, vol. 7, pp. 55–129.

Bazant, Z. P. & Oh, B. H., 1983. Crack band theory for fracture of concrete. *Material and Structures*, vol. 16, pp. 155–177.

Bazant, Z. P. & Pijadeur-Cabot, G., 1988. Non-local continuum damage, localization instabilities and convergence. *Journal of Applied Mechanics*, vol. 55, pp. 287–293.

Benzeggagh, M. L. and Kenane, M., 1996. Measurement of mixed-mode delamination fracture toughness of unidirectional glass/epoxy composites with mixed-mode bending apparatus. *Composites Science Technology*, vol. 56, pp. 439–449

Cendon, D. A., Galvez, J. C., Elices, M. & Planas, J., 2000. Modelling the fracture of concrete under mixed loading. *International Journal of Fracture*, vol. 103, pp. 293–310.

Davila, C. G., Camanho, P. P. & Turon, A., 2007. Cohesive elements for shells. *National Aeronautic and Space Administration*, NASA/TP-2007-214869.

Dugdale, D. S., 1960. Yielding of steel sheets containing slits. In: *Journal of Mechanics and Physics of Solids*, vol. 8, issue: 2, pp. 100–104.

Galvez, J. C., Cendon, D. A., Planas, J., Guinea, G.V. & Elices, D. A., 1998. Fracture of concrete under mixed loading experimental results and numerical prediction. *Fracture Mechanics of Concrete Structures*, Proceedings FRAMCOS-3. Vol. 2, pp. 729- 738.

Galvez, J. C., Cendon, D. A., & Planas, J., 2002. Influence of shear parameters on mixed–mode fracture of concrete. *International Journal of Fracture*, vol. 118, pp. 163–189.

Galvez, J.C., Elices, M., Guinea, G.V. & Planas, J., (1996. Crack trajectories under mixed mode and non-proportional loading. *Computers, Materials, & Continua*, vol. 9, pp. 51–92.

Galvez, J. C., Elices, M., Guinea, G.V. & Planas, J., 1998. Mixed mode fracture of concrete under proportional and nonproportional loading. *International Journal of Fracture*, vol. 94, pp. 267–284.

Gonzalvez, E. V., Maimi, P., Turon, A., Camanho, P. P. & Renart, J., 2009. Simulation of delamination by means of cohesive elements using an explicit finite element code. *International Journal of Fracture*, vol. 94, pp. 267–284.

Mejia, E. C., Paullo, L. F. & Roehl, D., (2015) Continuation methods for the simulation of rock fracture with cohesive elements, *ISRM Congress 2015 proceedings-Int'l Symposium on Rock Mechanics*, ISBN: 978-1-926872-25-4.

Park, K. & Paulino, G., 2012. Computational implementation of the PPR potential-based cohesive model in Abaqus: Educational perspective. *Engineering Fracture Mechanics*, vol. 93, pp. 239–262.

Park, K., Paulino, G. & Roesler, J. R., 2008. A unified potential-based cohesive model of mixed-mode fracture. *Journal of the Mechanics and Physics of Solids*, vol. 57, pp. 891–908.

Potts, D. M. & Zdravkovic, L., 1999. Finite elements analysis in geotechnical engineering – Theory, pp. 68-70. Thomas Telford.

Rabczuk, T., 2013. Computational methods for fracture in brittle and quasi-brittle solids: state-of-art review and future perspectives. *ISRN Applied Mathematics*, vol. 2013, pp. 38.

Reyes, E., Casati, M. J. & Galvez, J. C., 2008. Cohesive crack model for mixed mode fracture of brick masonry. *International Journal of Fracture*, vol. 151, pp. 29–55.

Turon, A., Camanho, P. P. & Davila, C. G., (2006) a damage model for the simulation of delamination in advanced composites under variable-mode loading. In: *Mechanics of Materials*, Elsevier, vol. 38, issue 11, pp. 1072-1089.